AMERICAN SOCIETY FOR MICROBIOLOGY | mBio®

RESEARCH ARTICLE

Cryptococcus neoformans Iron-Sulfur Protein Biogenesis Machinery Is a Novel Layer of Protection against Cu Stress

Sarela Garcia-Santamarina,[a] Marta A. Uzarska,[b] Richard A. Festa,[a]* Roland Lill,[b,c] Dennis J. Thiele[a,d,e]

Duke University School of Medicine, Durham, North Carolina, USA[a]; Institut für Zytobiologie & Zytopathologie, Philipps-Universität, Marburg, Germany[b]; LOEWE Zentrum für Synthetische Mikrobiologie SynMikro, Marburg, Germany[c]; Department of Pharmacology and Cancer Biology, Department of Biochemistry, Duke University School of Medicine, Durham, North Carolina, USA[d]; Department of Molecular Genetics and Microbiology, Duke University School of Medicine, Durham, North Carolina, USA[e]

ABSTRACT Copper (Cu) ions serve as catalytic cofactors to drive key biochemical processes, and yet Cu levels that exceed cellular homeostatic control capacity are toxic. The underlying mechanisms for Cu toxicity are poorly understood. During pulmonary infection by the fungal pathogen *Cryptococcus neoformans*, host alveolar macrophages compartmentalize Cu to the phagosome, and the ability to detoxify Cu is critical for its survival and virulence. Here, we report that iron-sulfur (Fe-S) clusters are critical targets of Cu toxicity in both *Saccharomyces cerevisiae* and *C. neoformans* in a manner that depends on the accessibility of Cu to the Fe-S cofactor. To respond to this Cu-dependent Fe-S stress, *C. neoformans* induces the transcription of mitochondrial ABC transporter Atm1, which functions in cytosolic-nuclear Fe-S protein biogenesis in response to Cu and in a manner dependent on the Cu metalloregulatory transcription factor Cuf1. As Atm1 functions in exporting an Fe-S precursor from the mitochondrial matrix to the cytosol, *C. neoformans* cells depleted for Atm1 are sensitive to Cu even while the Cu-detoxifying metallothionein proteins are highly expressed. We provide evidence for a previously unrecognized microbial defense mechanism to deal with Cu toxicity, and we highlight the importance for *C. neoformans* of having several distinct mechanisms for coping with Cu toxicity which together could contribute to the success of this microbe as an opportunistic human fungal pathogen.

IMPORTANCE *C. neoformans* is an opportunistic pathogen that causes lethal meningitis in over 650,000 people annually. The severity of *C. neoformans* infections is further compounded by the use of toxic or poorly effective systemic antifungal agents as well as by the difficulty of diagnosis. Cu is a natural potent antimicrobial agent that is compartmentalized within the macrophage phagosome and used by innate immune cells to neutralize microbial pathogens. While the Cu detoxification machinery of *C. neoformans* is essential for virulence, little is known about the mechanisms by which Cu kills fungi. Here we report that Fe-S cluster-containing proteins, including members of the Fe-S protein biogenesis machinery itself, are critical targets of Cu toxicity and therefore that this biosynthetic process provides an important layer of defense against high Cu levels. Given the role of Cu ionophores as antimicrobials, understanding how Cu is toxic to microorganisms could lead to the development of effective, broad-spectrum antimicrobials. Moreover, understanding Cu toxicity could provide additional insights into the pathophysiology of human diseases of Cu overload such as Wilson's disease.

KEYWORDS ABC transporters, copper toxicity, Cryptococcus neoformans, Fe-S cluster, copper ionophores, metalloproteins, mitochondria

Received 21 September 2017 **Accepted** 3 October 2017 **Published** 31 October 2017

Citation Garcia-Santamarina S, Uzarska MA, Festa RA, Lill R, Thiele DJ. 2017. *Cryptococcus neoformans* iron-sulfur protein biogenesis machinery is a novel layer of protection against Cu stress. mBio 8:e01742-17. https://doi.org/10.1128/mBio.01742-17.

Editor Michael Lorenz, University of Texas Health Science Center

Address correspondence to Roland Lill, Lill@staff.uni-marburg.de, or Dennis J. Thiele, dennis.thiele@duke.edu.

* Present address: Richard A. Festa, Irvine Scientific, Santa Ana, California, USA.

S.G.-S. and M.A.U. contributed equally to this article.

This article is a direct contribution from a Fellow of the American Academy of Microbiology. Solicited external reviewers: Daniel Kosman, University of Buffalo; Bernhard Hube, Leibniz Institute for Natural Product Research and Infection Biology - Hans Knoell Institute Jena, HKI.

Cryptococcus neoformans is a fungal pathogen that lives in the soil and on plants in the environment and which infects humans through inhalation. The lungs are the primary site of infection, where alveolar macrophages compartmentalize *C. neoformans* into the phagosome, a hostile environment that serves to dampen fungal growth and survival. *C. neoformans* cells that survive phagocytosis can escape macrophages through lytic or nonlytic exocytosis and can cause cryptococcal pneumonia or can enter the bloodstream and cross the blood-brain barrier, causing lethal meningitis (1–3). Each year, approximately 1 million cryptococcal infections are diagnosed, resulting in over 600,000 deaths per year, predominantly among immunocompromised individuals (4). Similarly to other opportunistic pathogens, *C. neoformans* must quickly adapt its life cycle to the constantly changing and challenging host microenvironments. Thus, the generation of a polysaccharide capsule, elaboration of enzymes such as melanin and urease, and the ability to adapt to excess or limited levels of factors required for growth are traits that influence the colonization, survival, and virulence of this organism within the host (5–8).

An important virulence trait that allows successful cryptococcosis is the ability of *C. neoformans* to sense and adapt to different host-driven copper (Cu) environments (9, 10). Cu is an essential transition metal required in many key biochemical processes, many of which are directly linked to virulence in *C. neoformans* (11). Thus, Cu is a cofactor for key enzymes involved in melanin formation, high-affinity Fe uptake, reactive oxygen species detoxification, and respiration (12–16). However, when present at high concentrations, Cu is also toxic. In this regard, *C. neoformans* Cu metalloregulatory transcription factor Cuf1 has been shown to be required for virulence, as it regulates the expression of genes required for both the acquisition and detoxification of Cu (17, 18). Under conditions of low Cu concentrations, Cuf1 activates the expression of genes encoding the *C*tr1 and Ctr4 Cu^+ transporters and cell surface metalloreductases which, together, drive Cu acquisition. In response to high environmental Cu concentrations, Cuf1 activates the expression of genes encoding the Cu-buffering metallothioneins Mt1 and Mt2 (17). Cuf1, Mt1/Mt2, and Ctr1/4 are all virulence factors in mouse models of cryptococcosis, and their requirement for virulence depends on the infectious niche (9, 10). In the brain, Ctr1 and Ctr4 are critical for Cu acquisition and cell survival (10). Within alveolar macrophages, however, *C. neoformans* Mt1/2 expression is critical for survival of the elevated Cu levels encountered in the phagosomal compartment (9).

It has recently been recognized that Cu is used by host innate immune cells as a potent microbicide. Using X-ray microprobe analysis, it was demonstrated that Cu concentrations increase in the phagosome of peritoneal macrophages infected with *Mycobacterium* spp. (19). Furthermore, activated macrophages coordinately increase expression of the Ctr1 Cu^+ importer at the plasma membrane and localize the ATPase ATP7A at the phagolysosomal membrane, resulting in the accumulation and compartmentalization of Cu in the phagosome (20). Defects in Cu^+ exporters or in metallothionein expression sensitize both bacterial and fungal pathogens to macrophage killing mechanisms that are dependent on the toxicity of Cu (20–23). However, the precise mechanisms whereby Cu is toxic to organisms remain incompletely understood. Classically, due to its redox properties, Cu-associated toxicity was attributed to an increase in the intracellular levels of reactive oxygen species, which irreversibly damage DNA, lipids, and/or proteins. More recently, Cu toxicity mechanisms were revisited and it has been suggested that iron-sulfur (Fe-S) cluster interference is a significant mechanism for Cu toxicity in bacterial cells (24, 25). Hence, recent *in vivo* and *in vitro* studies in *Escherichia coli* demonstrated that Cu targets solvent-exposed Fe-S clusters of dehydratases involved in the synthesis of branched-chain amino acids and the *E. coli* Fe-S cluster biogenesis protein IscA (24, 26). Additional work performed *in vitro* demonstrated that Cu^+ destabilizes Fe-S clusters from the bacterial SufU protein (27), the major scaffold used by the sulfur assimilation (SUF) system for Fe-S cluster assembly and transfer to target proteins, and from mammalian ISCA1/2 and GLRX5, mitochondrial proteins involved in Fe-S cluster trafficking (28).

Here we report that Fe-S cluster-containing proteins and the Fe-S protein assembly machinery itself are critical targets for Cu toxicity in *C. neoformans* and in *Saccharomyces cerevisiae*. In *S. cerevisiae*, Cu targets Fe-S clusters, including several components of the cytosolic Fe-S protein assembly (CIA) machinery, with sensitivity that depends on the solvent accessibility of the cofactor to Cu. Unexpectedly, *C. neoformans* responded to elevated Cu levels by activating the expression of the *ATM1* gene, encoding a mitochondrial ABC transporter that mobilizes a precursor for Fe-S biogenesis to the cytosol (29–31), in a Cuf1-dependent manner. Atm1 depletion resulted in a growth defect under conditions of Cu stress, even in the presence of the Cu-buffering metallothioneins. These results highlight the importance for *C. neoformans* of implementing several mechanisms for coping with Cu toxicity, which together could contribute to the survival of this pathogen in the presence of the host innate immune system.

RESULTS

Atm1, a predicted ABC transporter with functions in the ISC export machinery, is regulated by Cuf1 during Cu stress in *C. neoformans*. Given the importance of the Cu detoxification machinery in *C. neoformans* pulmonary infection (9), we characterized the transcriptome of *C. neoformans* in response to elevated Cu concentrations to identify additional pathways relevant for handling toxic Cu concentrations. One gene activated during Cu stress corresponds to *CNAG_04358*, which codes for a homologue of the previously characterized *S. cerevisiae* mitochondrial inner membrane ATP-binding cassette (ABC) transporter Atm1. In *S. cerevisiae*, this protein exports from the mitochondrial matrix to the cytosol an unknown, sulfur-containing component which is required for maintaining cellular Fe homeostasis and is utilized by the CIA machinery for maturation of cytosolic and nuclear Fe-S proteins (29, 30, 32). In *C. neoformans*, expression of genes in response to Cu limitation as well as Cu excess is dependent on metalloregulatory transcription factor Cuf1 (17). To ascertain whether *C. neoformans ATM1* expression during Cu stress is Cuf1 dependent, *ATM1* mRNA levels were analyzed and quantitative real-time reverse transcription-PCR (qRT-PCR) analysis of the wild-type strain, mutant Δ*Cuf1*, and a Δ*Cuf1* strain complemented with wild-type Cuf1 was performed (Fig. 1A). *ATM1* mRNA levels were significantly reduced in the Δ*Cuf1* strain compared with the parental wild-type and complemented Δ*Cuf1* strains. To further address whether *C. neoformans ATM1* belongs to the Cuf1 regulon, Cuf1 occupancy on the *ATM1* promoter was analyzed by chromatin immunoprecipitation-PCR (ChIP-PCR) in wild-type cells that were treated either with Cu or with the Cu chelator bathocuproine disulfonic acid (BCS) (Fig. 1B). The results showed that Cuf1 was significantly enriched at the *ATM1* promoter during Cu exposure compared to the results seen under conditions of Cu limitation. To validate that increased *ATM1* mRNA levels result in increased Atm1 protein levels, the Atm1 protein was fused with a carboxyl-terminal 4× FLAG epitope tag (Atm1-F) under the control of the native *ATM1* promoter to generate a functional fusion protein (see Fig. S1A in the supplemental material). After treatment with 1 mM Cu, Atm1-F levels, analyzed by immunoblotting, increased as early as 15 min after Cu stress and continued to accumulate for at least 90 min (Fig. 1C). Together, these results demonstrate that Cu enhances *C. neoformans* Cuf1-dependent *ATM1* expression both at the mRNA level and at the protein level.

Atm1 homologues are present in all eukaryotes and in some bacteria, with ~50% sequence identity among homologues from bacteria to humans (33). Multiple-sequence alignment performed with hierarchical clustering showed that this conservation is maintained within *Cryptococcus* spp. (Fig. S1B). We investigated whether *S. cerevisiae* Atm1 (*Sc*Atm1) expression is also induced under conditions of Cu stress in a fashion similar to that seen with *C. neoformans* Atm1 (*Cn*Atm1). Interestingly, *S. cerevisiae* cells treated with Cu showed no altered Atm1 expression (Fig. 1D), suggesting that the different organisms have intrinsically different ways to respond to Cu stress through Cu-regulated gene expression.

***C. neoformans* Atm1 functions in cytosolic iron-sulfur protein formation.** *Sc*Atm1 functions by exporting an Fe-S cluster precursor from the mitochondrial matrix

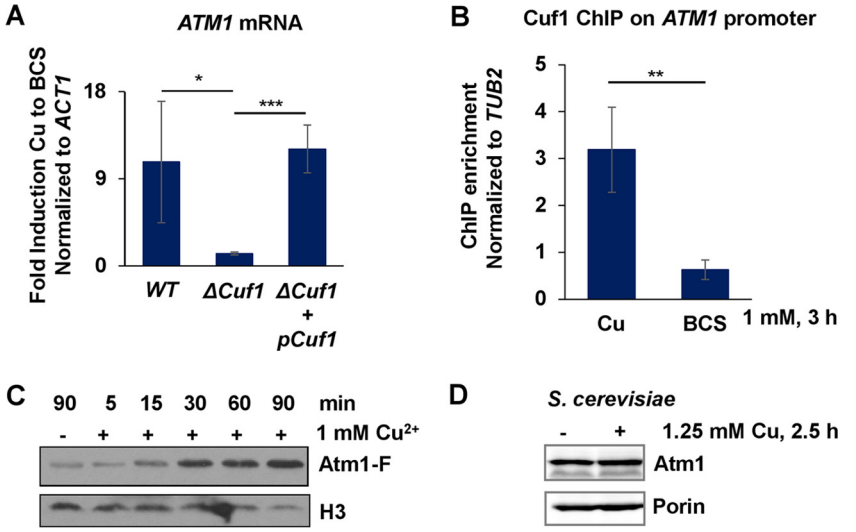

FIG 1 Expression of the mitochondrial ABC transporter Atm1 is induced by Cu in a Cuf1-dependent manner in *C. neoformans*. (A) Exponentially growing cultures of *C. neoformans* strains H99 (DTY758), Δ*Cuf1* (DTY761), and Δ*Cuf1* with complementing Cuf1 (DTY762) were treated with 1 mM BCS and 1 mM Cu for 3 h. Gene expression was analyzed by qRT-PCR with specific primers for *ATM1* and *ACT1* (used for data normalization). $n = 4$ (one-way repeated-measures ANOVA test, $P = 0.02$). (B) Exponentially growing cultures of *C. neoformans* strains Cuf1-FLAG (DTY762) and H99 (DTY758) were treated with 1 mM $CuSO_4$ or 1 mM BCS. ChIP was performed using anti-FLAG antibody, and Cuf1 occupancy was analyzed by qRT-PCR with primers for the promoter regions of the *ATM1* and *TUB2* genes. *C. neoformans* H99 was used as a negative control. $n = 3$ (Student's *t* test of paired samples, $P = 0.002$). (C) Cellular protein extracts were obtained from exponentially growing cultures of *C. neoformans* strain Atm1-F (DTY947) that had been left untreated (unt) or had been treated with 1 mM Cu during the indicated times and analyzed by SDS-PAGE and immunoblotting with antibodies against FLAG and histone 3 (H3; loading control). (D) *S. cerevisiae* Atm1 protein expression is not affected by Cu stress. Cellular protein extracts were obtained from untreated or Cu (1.25 mM)-treated exponentially growing cultures of *S. cerevisiae* strain W303A (wild type [WT]) and analyzed by SDS-PAGE and immunoblotting with antibodies against Atm1 and porin (loading control).

to the cytosol, which is used by the CIA machinery for the synthesis and maturation of cytosolic and nuclear Fe-S proteins (29, 30, 32). *S. cerevisiae* cells depleted of Atm1 have reduced growth rates and reduced activities of cytosolic and nuclear Fe-S cluster proteins and constitutively express a set of genes largely overlapping with the transcriptional response of yeast to Fe deficiency (34). As a consequence of the latter, *S. cerevisiae* cells lacking Atm1 accumulate iron in the mitochondria and have reduced levels of holo-heme proteins and increased levels of oxidative stress (30). To assess whether *Cn*Atm1 functions as a bona fide Atm1, *Cn*Atm1 was tested for complementation in *S. cerevisiae* strain GalL-Atm1, in which *ATM1* gene expression is under the control of the galactose-inducible and glucose-repressible *GALL* promoter. This strain was transformed with either an empty vector or a vector expressing *S. cerevisiae ATM1* or *C. neoformans ATM1*. As shown in Fig. S2A, *Cn*Atm1 rescued the growth of *S. cerevisiae* cells lacking Atm1 to an extent similar to that seen with cells expressing *Sc*Atm1. Similarly, the activity of the cytosolic Fe-S enzyme isopropyl malate dehydratase (Leu1) (Fig. S2B, left panel) was restored by expression of both *Sc*Atm1 and *Cn*Atm1, suggesting that the *C. neoformans* Atm1 protein is able to support the maturation of cytosolic Fe-S proteins. Moreover, *S. cerevisiae GalL-Atm1* cells depleted of endogenous *Sc*Atm1 and expressing *Cn*Atm1 increased activity of the heme-containing protein catalase compared to the results seen with the empty vector control, with no impact on a control enzyme (Fig. S2B, middle panel). As cells lacking Atm1 display disturbed iron homeostasis and increased the expression of the Aft1/Aft2 transcription factor-dependent iron regulon, we measured the expression of a reporter gene that is responsive to Fe deficiency (35, 36). Expression of both *Sc*Atm1 and *Cn*Atm1 in *S. cerevisiae* cells depleted of Atm1 severely decreased the activation of the Fe deficiency-responsive promoter (Fig. S2C).

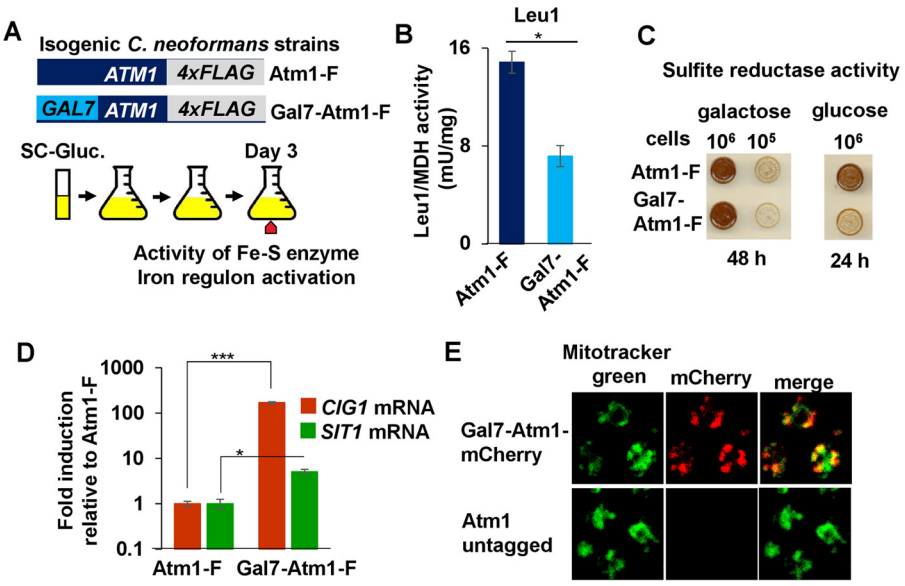

FIG 2 *C. neoformans* Atm1 is a functional ortholog of *S. cerevisiae* Atm1. (A) Scheme representing the steps for the experimental procedures performed as described for panels B to D. (B to D) Cultures of *C. neoformans* strains Atm1-F (DTY947) and Gal7-Atm1-F (DTY949) were back diluted in SC-Gluc media for 3 days. Cultures were diluted to the desired OD in SC-Gluc media and grown for 3 h, and the ratio of Leu1 (Fe-S enzyme) enzymatic activity to malate dehydrogenase (MDH) (lacking Fe-S clusters) enzymatic activity (B), the sulfite reductase activity (C), and the gene expression of *CIG1* and *SIT1* normalized to *ACT1* (D) were assayed. For Leu1/MDH activity analysis, $n = 3$ (Student's *t* test of paired samples, $P = 0.02$). For *CIG1*/*ACT1* expression analysis, $n = 3$ (Student's *t* test of paired samples, $P = 0.0007$). For *SIT1*/*ACT1* expression analysis, $n = 3$ (Student's *t* test of paired samples, $P = 0.02$). (E) *C. neoformans* Atm1 localizes to mitochondria. Strains Gal7-Atm1-mCherry (DTY951) and H99 (Atm1-untagged) were grown in SC-Gal media for 3 days and incubated with Mitotracker green (for mitochondrial staining) and Atm1-mCherry localization. Samples were analyzed by confocal microscopy.

We tested whether *C. neoformans* cells lacking Atm1 show phenotypes similar to those seen with the Atm1-deficient *S. cerevisiae* strain. The native promoter of the *C. neoformans* epitope-tagged Atm1-F allele was replaced with the *GAL7* promoter (Gal7-Atm1-F) (Fig. 2A). We used the *GAL7* promoter instead of generating a Δ*Atm1* strain to subvert the Cu-dependent and Cuf1-dependent expression of *ATM1* and to prevent permanent strain adaptations to the lack of Atm1, which is required for the maturation of cytosolic and nuclear Fe-S proteins, some of which are essential. As confirmed by qRT-PCR and by immunoblotting (Fig. S2D), the Gal7-Atm1-F strain showed high levels of *ATM1-F* transcript and protein in galactose and reduced levels in glucose compared to the expression of *ATM1-F* under the control of its native promoter. After the isogenic strains were grown for 3 days in glucose, the activities of the cytosolic Fe-S proteins Leu1 (Fig. 2B) and sulfite reductase (Fig. 2C) were significantly decreased in the Gal7-Atm1-F strain upon depletion of Atm1. Similarly, two *C. neoformans* genes, *CIG1* and *SIT1*, previously shown to be activated during Fe starvation (37), showed increased expression in the Gal7-Atm1-F strain compared to the Atm1-F strain (Fig. 2D). Since *S. cerevisiae* Atm1 localizes to the mitochondrial inner membrane (38), we determined the localization of a *Cn*Atm1-mCherry fusion protein. Confocal microscopy revealed colocalization of Atm1-mCherry with Mitotracker green, demonstrating that *C. neoformans* Atm1 is a mitochondrial protein (Fig. 2E, merge). Together, these results demonstrate that *C. neoformans* Atm1 is a bona fide functional orthologue of *S. cerevisiae* Atm1.

***C. neoformans* Atm1-depleted cells are more susceptible to Cu toxicity.** In *C. neoformans*, Cuf1-dependent activation of metallothionein genes *MT1* and *MT2* in response to Cu stress is crucial for survival within the host lungs, the primary site of infection (9). Since Atm1 expression is also activated in a Cuf1-dependent manner during Cu stress, we ascertained whether Atm1 is important for cell survival under

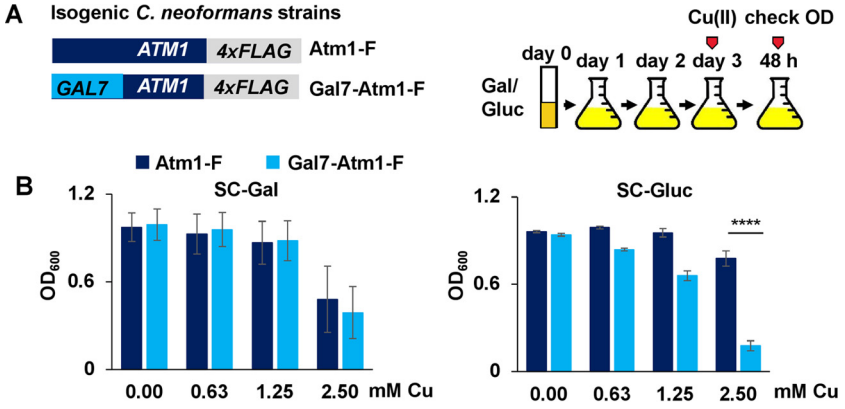

FIG 3 *C. neoformans* cells expressing low Atm1 protein levels are more sensitive to Cu stress than wild-type cells. (A) Scheme representing steps for the experimental procedures performed as described for panel B. Cultures of *C. neoformans* strains Atm1-F (DTY947) and Gal7-Atm1-F (DTY949) were diluted in either galactose-containing media or glucose-containing media for 3 days and diluted into 96-well plates to an OD of 0.002 in galactose-containing media or glucose-containing media, respectively, with the indicated concentrations of Cu. The final OD was recorded after 48 h. (B) Cultures of *C. neoformans* strains prepared as shown in panel A were grown in SC-Gal media (left panel) or in SC-Gluc media (right panel) with the indicated amounts of Cu. $n = 3$ (3-way repeated-measures ANOVA test). Cu differentially impacted growth of the strains only in the presence of glucose ($P < 0.0001$).

conditions of high Cu concentrations. The Atm1-F and Gal7-Atm1-F strains were grown for 3 days either in galactose or glucose, diluted into 96-well plates, and grown with or without additional Cu (Fig. 3A). *C. neoformans* cells lacking Atm1 (Gal7-Atm1-F cells grown in glucose) exhibited a growth defect in the presence of Cu compared with cells expressing Atm1 under the control of the native promoter (Atm1-F) (Fig. 3B, right panel). This growth defect was not observed when the strains were grown in galactose as a carbon source (Fig. 3B, left panel). These results could be explained by decreased expression of the *MT1/2* genes upon Atm1 depletion. However, as shown in Fig. S3A, the *MT1/2* genes are induced several-hundred-fold, independently of Atm1 expression. *S. cerevisiae* Δ*Atm1* cells have a severe growth defect. On the basis of the functional similarity of Atm1 proteins from the two yeasts, we anticipated that Atm1-depleted *C. neoformans* cells would display a similar growth phenotype. Interestingly, even though the Atm1 protein was undetectable by immunoblotting in the Gal-Atm1-F strain after growth in glucose (Fig. S2D), this strain displayed only a slight growth defect, and that growth defect was no longer significant after 48 h, compared with the results seen with the Atm1-F strain in the absence of Cu stress. This phenotype could be attributed to a requirement for only low levels of Atm1 protein or to a compensatory function of another mitochondrial ABC transporter, Mdl1, both of which are effects previously described for *S. cerevisiae* (30, 33, 39).

Components of yeast media, such as the amino acids cysteine, methionine, and histidine, along with other thiol-containing compounds, can chelate Cu (40). Since *C. neoformans* grows in minimal media lacking these nutrients, we ascertained whether the Cu sensitivity phenotype shown by Atm1-depleted cells would be enhanced if the cells were grown in a medium with lower levels of Cu chelation properties. As shown in Fig. S3B, right panel, the Gal7-Atm1-F strain grown in glucose medium (i.e., with undetectable Atm1 expression) and in the absence of exogenous amino acids was about 30-fold more sensitive to Cu stress than the same strain grown in the presence of amino acids (Fig. S3B, right panel), suggesting that Cu buffering is important in preventing Cu toxicity in the absence of Atm1. To test whether the role of Atm1 in Cu toxicity would be additive with respect to that of the metallothioneins, the *GAL7-ATM1* allele was placed into a *C. neoformans* Δ*Mt1* Δ*Mt2* strain (Δ*Mt1* Δ*Mt2* Gal7-Atm1). The Δ*Mt1* Δ*Mt2* and Δ*Mt1* Δ*Mt2* Gal7-Atm1 strains were grown in galactose or glucose and in the presence or absence of Cu stress. Atm1-depleted cells (Fig. S3C) showed significantly reduced growth in the presence of Cu compared to cells expressing Atm1

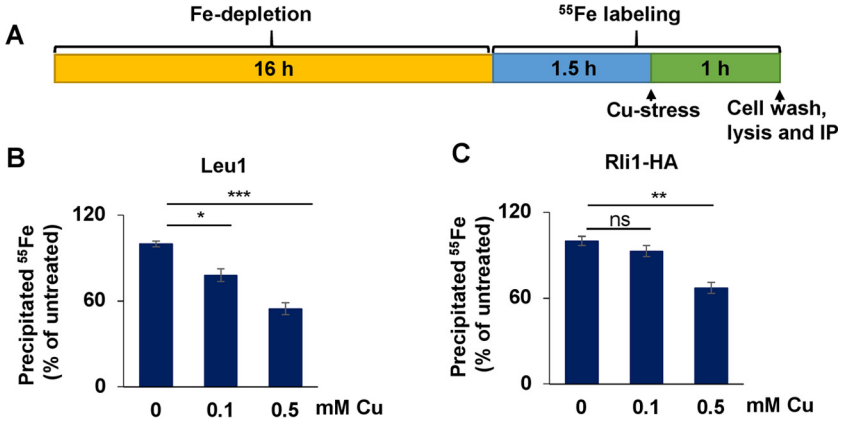

FIG 4 Cu targets cytosolic solvent-exposed Fe-S clusters. (A) Experimental setup for ^{55}Fe labeling experiments. Cells were grown for 16 h in Fe-poor SC medium with glucose and radiolabeled with 10 μCi ^{55}Fe for 1.5 h, $CuSO_4$ was added, and cells were grown in the presence of both ^{55}Fe and Cu for 1 h. (B) Wild-type (WT) *S. cerevisiae* cells were grown as described for panel A. Endogenous Leu1 protein was immunoprecipitated from cell extracts with specific antibodies. The amount of coprecipitated ^{55}Fe was quantified by scintillation counting. Data are presented relative to the values obtained for samples not treated with Cu. $n = 8$ (one-way repeated-measures ANOVA test, $P < 0.0001$). (C) WT cells transformed with vector overproducing Rli1-HA were grown as described for panel A and processed as described for panel B. $n = 8$ ($P = 0.005$).

from the native promoter, with increased Cu sensitivity of the Δ*Mt1* Δ*Mt2* Gal7-Atm1 strain to Cu compared to a Gal7-Atm1-F strain (compare Fig. 3B to S3C). This suggests that the role of Atm1 in preventing Cu toxicity is complementary and additive with respect to the Cu sequestration function of the *C. neoformans* metallothioneins.

Fe-S proteins are targets of Cu toxicity in *S. cerevisiae*. Previous studies have implicated Fe-S proteins among the targets of Cu toxicity. These studies showed that Cu displaces Fe ions from solvent-exposed Fe-S clusters, suggesting that Cu(I) damages Fe-S proteins by directly binding to the coordinating sulfur atoms (24, 26–28). Thus, we sought to determine if Cu might also damage Fe-S clusters in *S. cerevisiae* using an *in vivo* ^{55}Fe incorporation method for detection of Fe-S clusters (Fig. 4A). Wild-type cells were incubated in Fe-poor medium for 16 h to deplete cells of Fe and to allow boosting of ^{55}Fe-S cluster incorporation into apoproteins. After an initial 1.5 h of ^{55}Fe labeling, cells were incubated with Cu for 1 h, washed, and lysed, and clarified lysates were subjected to immunoprecipitation performed with specific antibodies. The precipitated ^{55}Fe radioactivity was quantified by scintillation counting.

We first tested whether two cytosolic Fe-S proteins, Leu1 and Rli1, were affected by Cu treatment. While structural studies demonstrated that Leu1 possesses a solvent-exposed [4Fe-4S] cluster (41), the two [4Fe-4S] clusters of the essential protein Rli1 were occluded from solvent (42, 43). In both cases, there was a significant decrease in the ^{55}Fe counts in the presence of Cu, in a dose-dependent fashion, with no change in steady-state protein levels (Fig. 4B and C and S4A and B). Significantly, while incubation of *S. cerevisiae* cells with 0.1 mM Cu was sufficient to produce a significant impact on ^{55}Fe-S associated with Leu1 (Fig. 4B), 0.5 mM Cu was required for a similar diminution of the Rli1 Fe-S clusters (Fig. 4C), suggesting that Cu was more effectively targeting solvent-exposed Fe-S clusters. Similarly, the Leu1 enzymatic activity was reduced by ~50% after 2.5 h of stress performed with 1.25 mM Cu (Fig. S4C). As mitochondria represent the primary site of synthesis of the Fe-S cluster precursor exported by Atm1 (35), we tested the effects of Cu stress on mitochondrial Fe-S proteins. The [4Fe-4S] cluster in aconitase (44) (Fig. S4D, left panel) and the [2Fe-2S] cluster of ectopically expressed human ferredoxin (45) (Fig. S4E, left panel), both solvent exposed, required 0.5 mM Cu to produce a weak and yet significant decrease in the level of the protein-associated ^{55}Fe-S cluster. The aconitase activity was affected only minimally after exposure to 1.25 mM Cu stress for either 2.5 h or 16 h (Fig. S4D, middle and right

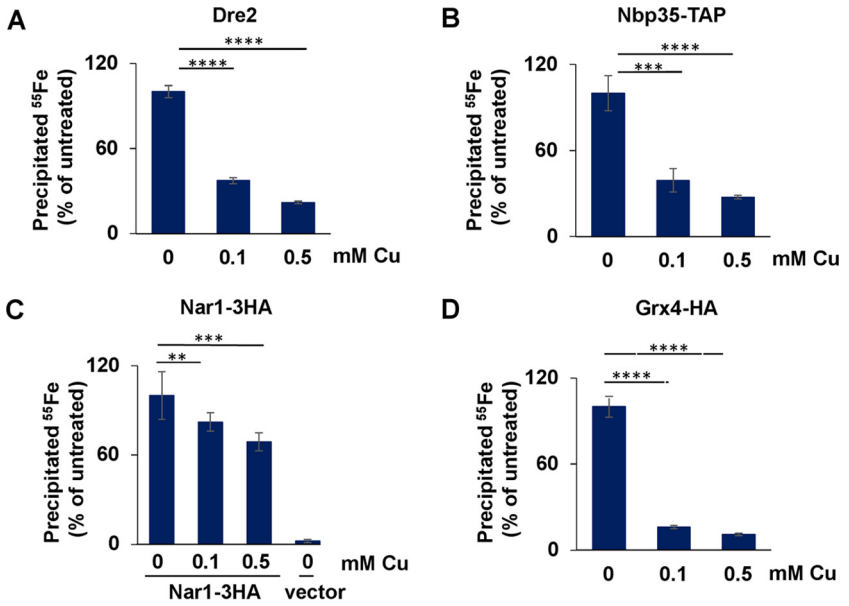

FIG 5 Critical targets for Cu toxicity are Fe-S clusters of proteins with functions in the CIA machinery and iron regulon activation. (A to D) WT *S. cerevisiae* cells (A), WT cells transformed with vector overproducing Nbp35-TAP (B) or Nar1-3HA (C), and WT cells in which the *GRX4* gene was genomically tagged with the HA epitope (D) were grown as described for Fig. 4A. The overproduced Nbp35-TAP and Nar1-3HA or endogenous Dre2 and Grx4-HA proteins were immunoprecipitated from cell extracts with specific antibodies. The amount of coprecipitated ^{55}Fe was quantified by scintillation counting. Data are presented relative to the values obtained for samples not treated with Cu. $n = 6$ for Nar1 and $n = 8$ for the remaining proteins (one-way repeated-measures ANOVA test, $P < 0.0001$ for Dre2, Nbp35, Nar1, and Grx4).

panels). Moreover, the Fe-S cluster of endogenous mitochondrial ferredoxin Yah1 was not affected by Cu stress at the concentrations of the metal tested (Fig. S4E, right panel). This is in contrast with the results from a recent publication in which ^{55}Fe incorporation into the Yah1 Fe-S cluster was reported to have been significantly diminished after 1 mM Cu treatment (46). The disparity could be attributed to differences in the ^{55}Fe immunoprecipitation experiments. We usually observe amounts of ^{55}Fe associated with immunoprecipitated Yah1 (or other Fe-S cluster binding proteins) that are at least 100-fold lower than the published data (46). Moreover, a disruption of the Yah1 Fe-S cluster should be accompanied by a lack of Fe-S clusters associated with Isu1 (47), Nar1, or Rli1; no such result was seen in the previous report (46). Collectively, our results suggest that mitochondrial Fe-S proteins are more resistant to Cu toxicity than those in the cytoplasm or nucleus.

As stronger defects were observed for cytosolic solvent-exposed Fe-S proteins than for mitochondrial Fe-S proteins, we investigated whether Cu could affect Fe-S clusters bound to CIA components (either transiently bound for subsequent insertion onto client apoproteins or permanently bound and required for function). If Cu disrupts Fe-S clusters in such CIA proteins, this may cause a decline in the assembly of cytosolic and nuclear apoproteins (48). In testing ^{55}Fe incorporation into the CIA protein Dre2 (49) (Fig. 5A) and the Fe-S scaffold protein Nbp35 (50) (Fig. 5B), we unexpectedly observed that both proteins were significantly more severely affected than the cytosolic client proteins Leu1 and Rli1 (compare to Fig. 4). In contrast, the Fe-S clusters of Nar1 (51) (Fig. 5C) were more stable than those of Dre2 and Nbp35. The concentrations of all of those proteins did not change during the course of the treatment (Fig. S5A to C). Precise structural information on these CIA proteins is still missing, but the Fe-S clusters are expected to be solvent accessible in Dre2 and Nbp35, and yet Nar1 may contain both a solvent-exposed cluster and a buried cluster (51).

In order to delve into the mechanism accounting for the fact that the Fe-S clusters from cytosolic CIA client proteins were more stable than those from the CIA machinery,

we investigated Fe-S cluster stability in Leu1 and Rli1 when the ^{55}Fe incorporation was performed in the presence of Cu. We envisioned that if Cu were present at the time of Fe-S cluster assembly, this would have a higher impact on cytosolic and nuclear targets. Thus, after 2 h of initial Cu stress, cells were labeled with ^{55}Fe during 2 h together with the presence of Cu (i.e., 4 h of Cu stress in total) before cell washing, lysis, immunoprecipitation with specific antibodies, and counting of immunoprecipitated ^{55}Fe were performed (Fig. S5E). Unexpectedly, we observed an impact on ^{55}Fe-S associated with Leu1 (Fig. S5F, left panel) and Rli1 (Fig. S5G) similar to that seen when proteins were preloaded with a ^{55}Fe-S cluster before Cu stress. Similarly, the decrease in enzymatic activity of Leu1 (Fig. S5F, right panel) seen upon 2.5 h of Cu stress was not further exacerbated by longer (16-h) Cu exposure (compare Fig. 4B and C). Surprisingly, the level of Fe-S biosynthetic activity of the CIA machinery was still high enough to partially assemble cytosolic Fe-S proteins in the presence of Cu. This is in agreement with previous *in vitro* experiments showing that, independently of transfer of Fe-S clusters through protein-protein interactions, the presence of excess Cu results in displacement of Fe from those Fe-S clusters for which it has higher binding affinity (28).

Finally, the effects of Cu stress on the Fe-S cluster of the cytosolic monothiol glutaredoxin Grx4 was evaluated (Fig. 5D). Grx4 has established roles in maintaining iron homeostasis in the cell and in assisting cytosolic-nuclear Fe-S protein biogenesis (35, 52). Grx4 possesses a solvent-exposed, bridging glutathione (GSH)-coordinated [2Fe-2S] cluster (53). Treatment with 0.1 mM Cu resulted in a pronounced decrease in ^{55}Fe binding (Fig. 5D) without any change in the protein concentration (Fig. S5D). When the Grx4 Fe-S site is unoccupied, this leads to activation of the iron regulon via the Aft1/2 transcription factors (54, 55). Surprisingly, although Fe binding by Grx4 was strongly decreased upon Cu treatment, the iron regulon was not activated, even when the cells were treated with Cu overnight (data not shown). How this happens will require further exploration, but cells could be implementing a mechanism to prevent additional oxidative stress that would be caused by Fe influx. As a further test of the functional state of the Fe-S protein biogenesis machinery, we evaluated Isu1 protein levels, which are elevated by protein stabilization even during slight perturbations of the ISC machinery (56, 57) (M. A. Uzarska, unpublished observation). We observed an increase in Isu1 levels at Cu concentrations that destabilize solvent-exposed Fe-S clusters (Fig. S5H), further suggesting that Cu perturbs the function of the Fe-S protein assembly machinery. Taken together, in agreement with studies in bacteria, these results suggest that Cu differentially affects the stability and/or assembly of Fe-S proteins in eukaryotic cells. Cytosolic Fe-S proteins are more sensitive to Cu than mitochondrial ones, especially the Fe-S cluster-containing CIA proteins and Grx4, even though they maintain partial efficiency with respect to assembly of cytosolic Fe-S proteins.

***C. neoformans* Fe-S cluster homeostasis during Cu stress.** Given that *C. neoformans* Atm1 is a functional orthologue of *S. cerevisiae* Atm1, the Cu-induced Cuf1-dependent activation of *C. neoformans* Atm1 expression could be a mechanism aimed at maintaining cytosolic and nuclear Fe-S cluster homeostasis during Cu stress. To address this hypothesis, we first measured ^{55}Fe incorporation into the *C. neoformans* Rli1 homologue fused to the hemagglutinin (HA) epitope tag in the Atm1-F- and Atm1-depleted Gal7-Atm1-F strains in the presence or absence of Cu stress, according to the scheme shown in Fig. 4A. As shown in Fig. 6A, levels of ^{55}Fe associated with Rli1 decreased with increasing Cu concentrations, while Rli1 protein levels remained unaltered in both strain backgrounds (Fig. S6A). Rli1 is among the most highly conserved proteins in nature, with two [4Fe-4S] clusters occluded from the solvent (42, 43). On the basis of published results from Cu toxicity experiments performed to analyze proteins with buried Fe-S clusters *in vitro* (24, 28) and of our data in Fig. 4C, we predicted that it would be difficult for Cu to directly target the Rli1 Fe-S clusters, and the decrease of the level of ^{55}Fe associated with Rli1 might more likely reflect the effect of the presence of functionally compromised CIA machinery during Cu stress. Atm1 depletion slightly

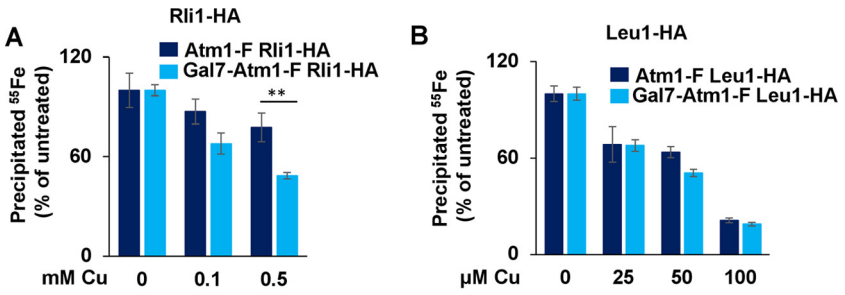

FIG 6 *C. neoformans* Atm1 contributes to the maintenance of cytosolic Fe-S cluster homeostasis during Cu stress. (A) Atm1-F Rli1-HA (DTY955) and Gal7-Atm1-F Rli1-HA (DTY957) *C. neoformans* cells were grown for 88 h in SC-Gluc medium to deplete Atm1 protein levels. During the last 16 h, cells were grown in Fe-poor SC-Gluc medium, and cells were radiolabeled with 10 μCi ^{55}Fe for 1.5 h before Cu was added and cells were incubated in the presence of both ^{55}Fe and Cu for 1 h (see Fig. 4A). Rli1-HA protein was immunoprecipitated from cell extracts with specific antibodies. The amount of coprecipitated ^{55}Fe was quantified by scintillation counting. Data are presented relative to the values obtained for samples not treated with Cu. $n = 4$ (two-way repeated-measures ANOVA test, $P = 0.04$). (B) Atm1-F Leu1-HA (DTY959) and Gal7-Atm1-F Leu1-HA (DTY961) *C. neoformans* cells were experimentally processed and analyzed as described for panel A. $n = 4$ (two-way repeated-measures ANOVA test, $P = 0.1$).

enhanced the loss of ^{55}Fe in Rli1-HA upon Cu stress compared with the isogenic strain with wild-type Atm1 protein levels (Fig. 6A). However, Atm1 depletion did not influence the amount of ^{55}Fe associated with Rli1 in an experiment in which Cu stress was applied before ^{55}Fe-S cluster assembly as schematized in Fig. S5E (Fig. 6SB), rendering a direct function of Atm1 in protecting Rli1 Fe-S cluster loading unlikely.

Along the same lines, although the levels of ^{55}Fe associated with *C. neoformans* Leu1-HA decreased upon Cu stress whereas the protein levels remained unchanged (Fig. 6B and C), this decrease was unaffected by Atm1 depletion. The disruption of the Leu1 Fe-S cluster by Cu had an impact on Leu1 enzymatic activity, and yet this effect was not significantly exacerbated by a depletion of Atm1 (Fig. S6D).

The weak or absent influence of Atm1 on the protection of the Fe-S clusters of these two cytosolic proteins suggests that their Fe-S clusters are not responsible for the strong Cu effect on the growth of Atm1-deficient cells (cf. Fig. 3 and S3). We therefore speculate that Cu might affect other essential cytosolic and/or nuclear proteins that require Atm1 for function, such as the Fe-S cluster-containing DNA polymerases, primases, and ATP-dependent helicases or the iron protein ribonucleotide reductase (32, 58).

We tested whether the toxic effect exerted by Cu on Atm1-depleted cells could be potentiated using zinc-pyrithione (ZPT), a small-molecule Cu ionophore that has potent antifungal properties and which was previously shown to cause damage to Fe-S clusters in proteins as part of its mechanism of action (59, 60). ZPT is an ionophore that rapidly exchanges the Zn(II) with a Cu(II) ion for which it has higher affinity. The mechanism of Cu-pyrithione action is not fully understood, but, potentially, it releases Cu within the cell, as supported by the ability of this compound to potently activate the Cu regulon (59, 60) (Fig. S7A). To test the toxicity of ZPT in *C. neoformans* cells depleted for Atm1, Atm1-F and Gal7-Atm1-F strains were grown in galactose or glucose, diluted into 96-well plates, and treated with increasing concentrations of ZPT (Fig. S7B). While there was no discernible difference in the growth rates of cells expressing Atm1 from the native promoter and of cells expressing Atm1 from the Gal7 promoter on synthetic complete galactose medium (SC-Gal) (Fig. S7A), Atm1-depleted cells did not grow in concentrations as low as 0.01 μM ZPT, a concentration at least 100-fold lower than that required for preventing the growth of cells expressing Atm1 from the native promoter (Fig. 7B; SC-Gluc). We ascertained whether the growth differences between Atm1-F and Gal7-Atm1-F on glucose medium were accompanied by differences in the activities of Fe-S proteins. Leu1 activity was tested after treatment of cells with 0.1 μM ZPT in the presence of 10 μM Cu. As shown in Fig. S7C, cells depleted of Atm1 had significantly reduced Leu1 activity upon ZPT and Cu treatment compared with the Leu1 activity

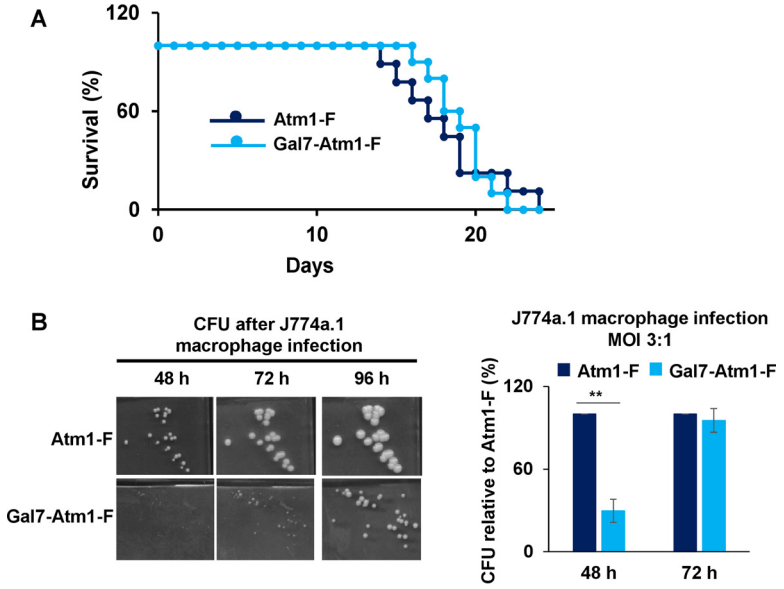

FIG 7 *C. neoformans* Atm1-depleted cells have decreased fitness upon coincubation with macrophage-like cell lines. (A) *C. neoformans* Atm1-depleted cells showed a trend toward reduced virulence in an intranasal mouse model of cryptococcosis. Cultures of strains Atm1-F (DTY967) and Gal7-Atm1-F (DTY969) were grown in SC-Gluc medium for 2 days and inoculated intranasally into two groups of 10 A/J mice with an inoculum size of 10^5 cells per mouse. Survival data are represented in a Kaplan-Meier plot, and statistical analysis was performed with the log-rank test ($P = 0.82$). (B) Cultures of strains prepared as described for panel A were grown in SC-Gluc medium for 2 days, diluted to 5×10^5 cells per ml in Dulbecco's modified Eagle's medium (DMEM), opsonized, and coincubated with the activated J774a.1 murine macrophage-like cell line at a multiplicity of infection (MOI) of 3:1. After the coincubation period, *C. neoformans* colonies were plated in SC-Gluc medium and representative pictures were taken at the indicated times (left panel). CFU counts were determined after 48 h or 72 h of incubation at 30°C and are presented relative to the data obtained for the Atm1-F strain (right panel). $n = 3$ (two-way repeated-measures ANOVA test, $P = 0.03$).

seen in Atm1-F cells. Interestingly, Leu1-HA protein levels decreased in Atm1-F cells in a parallel experiment under conditions of treatment with ZPT and Cu (Fig. S7D), suggesting that the recovered Leu1 activity in Atm1-F cells after 2 and 4 h of treatment could have been due to an Fe-S cluster repair mechanism driven by Atm1. However, the decrease in Leu1 activity alone cannot explain the differences in lethality between Atm1-expressing cells and Atm1-deficient cells, suggesting that either an essential Fe-S protein or a combination of effects in several Fe-S proteins was being targeted by the Cu ionophore.

Low levels of Atm1 impact *C. neoformans* fitness in macrophages and mice. The *C. neoformans* Cu-buffering metallothioneins are virulence factors in intranasal mouse models of cryptococcosis (9). On the basis of the observed growth defect of *C. neoformans* Atm1-depleted cells upon Cu exposure, we hypothesized that this Cu sensitivity could compromise *C. neoformans* growth during host colonization. To test the contribution of Cu-dependent expression of Atm1 to virulence, intranasal mouse infections were conducted with the Atm1-F and Gal7-Atm1-F strains after 2 days of Atm1 depletion in glucose. As shown in Fig. 7A, there was a modest, though not statistically significant, decrease in Gal7-Atm1-F strain virulence compared to that seen with the wild type. However, we could not assess whether Atm1 levels were maintained or repressed during the course of the *in vivo* infection in the *GAL7* promoter-controlled strain. Furthermore, these strains are still able to induce expression of *MT1/2*, which are by far the main factors contributing to Cu detoxification in this fungus.

In order to further assess the contribution of Atm1 to virulence, but in a more controlled system, we explored whether Atm1 depletion would affect growth of *C. neoformans* cells after macrophage phagocytosis. Host innate immune cells such as macrophages use Cu as a microbiocidal agent against microbial pathogens by accu-

mulating and compartmentalizing the metal into the phagosome. Lipopolysaccharide (LPS)- and gamma interferon (IFN-γ)-activated macrophages coordinately increase the expression of both the high-affinity Cu^+ importer Ctr1 at the plasma membrane and the Cu^+-transporting P-type ATPase, ATP7A, at the phagolysosomal membrane (20). We used the J774a.1 macrophage-like cell line and infected it with *C. neoformans* Atm1-F and Gal7-Atm1-F strains, the latter depleted for Atm1 by growth in glucose for 2 days. J774a.1 cells were activated with LPS and IFN-γ for 24 h and then independently infected with the two *C. neoformans* strains opsonized with the monoclonal 18B7 antibody. After 2 h, nonphagocytosed *C. neoformans* cells were washed away and J774a.1 cells with phagocytosed *C. neoformans* cells were further incubated for an additional 24 h before lysing of macrophages and plating of fungal cells for measuring CFU levels were performed. As shown in Fig. S8, the two strains were equally phagocytosed by the J774a.1 cells. However, as shown in Fig. 7B, CFU recovered from the Gal7-Atm1-F strain represented a significant growth delay compared with CFU recovered from the Atm1-F strain. Even though the colony remained smaller for the Gal7-Atm1-F strain, the number of CFU matched that of the wild-type Atm1-F strain, detected after 72 h of incubation at 30°C. These results suggest that macrophages cause higher levels of stress in Atm1-depleted *C. neoformans* than in wild-type cells, with the consequences of this stress being fungistatic rather than fungicidal.

DISCUSSION

While the toxicity of Cu as an antimicrobial agent has been harnessed for centuries, our understanding of the mechanisms of Cu antimicrobial activity against cell growth is surprisingly poor. Given the role of Cu ionophores as antimicrobials, and the requirement for Cu for innate immune cell function in coping with infections, a better understanding of what causes Cu to be toxic to microorganisms could lead to the development of effective, broad-spectrum antimicrobials. Moreover, understanding fundamental aspects of Cu toxicity is likely to provide additional insights into the pathophysiology of human diseases of Cu overload such as Wilson's disease.

Previous work demonstrating the importance of Cuf1, the Cu^+ transporters, and metallothioneins in virulence in different host infectious niches supports a role for both Cu acquisition and Cu detoxification in the *C. neoformans* infectious journey (9, 10). While the Mt1 and Mt2 proteins are powerful Cu sequestration tools that *C. neoformans* uses for Cu detoxification, we demonstrate in this work that the Cuf1- and Cu-dependent activation of the mitochondrial ABC transporter Atm1 is a novel additional mechanism used by this organism to cope with Cu toxicity. Cells expressing Atm1 grew much better in the presence of increasing levels of Cu than cells in which Atm1 was downregulated (Fig. 3B, left and right panels). Previous studies in yeast, mouse, humans, and plants firmly established the structure and function of Atm1 as a critical exporter of a precursor in the Fe-S cluster biogenesis pathway (30, 35, 61). Here, we confirm the function of *C. neoformans* Atm1 in cytosolic Fe-S protein biogenesis.

While Rli1 with its two stably bound [4Fe-4S] clusters (62, 63) and the [4Fe-4S] hydratase Leu1 were differentially sensitive to increasing levels of Cu, the additional depletion of Atm1 did not consistently further diminish the Fe-S cluster content in these two proteins. This finding was independent of whether Fe-S cluster assembly was tested (Cu addition before the ^{55}Fe assay) or whether the Fe-S cluster stability was analyzed (^{55}Fe-S cluster generated before Cu addition). We therefore postulate that other Atm1-dependent cytosolic and/or nuclear Fe-S proteins or the iron protein ribonucleotide reductase (58) might be responsible for the strongly increased growth defect of Atm1-depleted cells seen in the presence of Cu. Fe-S candidate proteins are DNA polymerases and primases or the ATP-dependent DNA helicases (32). Hence, future studies need to identify and analyze these essential Fe-S proteins to ascertain which of them might be responsible for the growth defect of Atm1-depleted cells in the presence of toxic concentrations of Cu. Nevertheless, cytosolic solvent-exposed Fe-S clusters seem to be perturbed by Cu by a combination of mechanisms. First, the solvent-exposed environment allows Cu to directly disrupt the cofactor, similarly to the

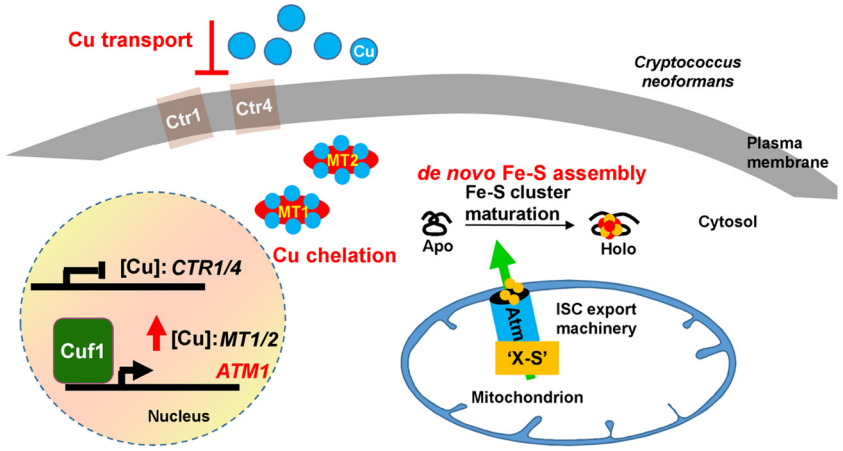

FIG 8 Model for the role of Atm1 during Cu stress in *C. neoformans*. In *C. neoformans*, Cuf1 is the primary transcription factor that regulates the expression of genes required for maintaining Cu homeostasis, either when Cu is scarce or when the concentrations approach toxic levels. When Cu concentrations approach toxic levels, Cuf1 occupancy is no longer enriched at promoters of genes with roles in Cu acquisition, as exemplified by the Cu importers Ctr1 and Ctr4, preventing the acquisition of more Cu^{+} from the environment. At the same time, Cuf1 occupancy is enriched at the *MT1* and *MT2* promoters, inducing the expression of the Mt1 and Mt2 proteins which sequester Cu, as they have high affinity and high binding capacity for this metal. The Cuf1-dependent and Cu-dependent induction of the expression of the mitochondrial ABC transporter Atm1 with a role in cytosolic and nuclear Fe-S protein biogenesis provides a novel way for coping with Cu toxicity. Fe-S proteins, which have many important and essential cellular functions, are major targets for Cu toxicity. Cu activation of Atm1 expression contributes to preservation of the homeostasis of cytosolic-nuclear Fe-S proteins, in particular, those with essential cellular functions, in the presence of toxic amounts of this metal.

effect of Cu in the Fe-S clusters from bacterial dehydratases. We note, however, that Leu1 seems to be much less severely and less selectively affected than bacterial enzymes (24). Second, the striking functional impairment of the Fe-S proteins of the CIA machinery observed in our study may delay the *de novo* assembly of the cofactor, at least in some (still unknown) sensitive Fe-S proteins. This may be the reason that *C. neoformans* increases Atm1 expression as an attempt to maintain essential cellular functions that depend on Fe-S clusters.

We have shown in this study that one of mechanisms of Cu toxicity in fungi is alteration of Fe-S cluster homeostasis in the cell by direct disruption of cofactor binding to target proteins. Our detailed analysis of the effects of Cu on different cellular Fe-S proteins revealed that the most Cu-sensitive Fe-S proteins contain a transiently bound or solvent-exposed cluster. Unexpectedly, the effect of Cu stress on Fe-S cluster disruption was more pronounced in members of the CIA machinery than in two analyzed downstream clients. A plausible explanation could be inferred from *in vitro* data from a recent report (28). In that work, it was shown that Fe-S clusters can be transferred through protein-protein interactions to downstream Cu-bound targets. However, very interestingly, the higher thiophilicity of the released Cu seen upon Fe-S transfer would immediately disrupt the newly formed Fe-S cluster. In this way, neither the transferring protein nor the downstream target would retain the Fe-S cluster. Similarly, in spite of a high level of Fe-S cluster loss in Grx4, there was no activation of the Fe regulon. On the basis of a report where the DNA-binding activity of the Fe-responsive transcription factor Aft2 was explored *in vitro* (54), both Fe^{2+} metals and other divalent metals, such as Cd^{2+} metals, were able to disrupt the DNA binding activity of the transcription factor. Thus, it is possible that either Fe released from the Cu-disrupted Fe-S clusters or Cu itself could bind this transcription factor and its homolog Aft1 to prevent active transcription of their target genes.

C. neoformans is an environmental fungus and an opportunistic pathogen. For a successful life cycle, this organism requires a degree of plasticity for fast adaptation to different environments (7). In the case of Cu, environmental challenges might have

favored the evolution of several layers of mechanisms for protecting *C. neoformans* from Cu stress, including an adaptation to both Cu deprivation and Cu toxicity (Fig. 8). When Cu levels approach toxic concentrations, *C. neoformans* prevents more Cu import into the cells by modifying both the localization and the stability of the Cu importers Ctr1 and Ctr4 at the plasma membrane, together with the release of Cuf1 from the Cu importer promoters (10, 17). Additionally, Cuf1 is enriched at the *MT1* and *MT2* promoters, inducing the expression of these cysteine-rich proteins, which can bind up to 16 and 24 atoms of Cu per protein, respectively (64). Despite the strong Cu-buffering capacity of the Mt proteins, this may be insufficient, and an additional Cuf1-dependent mechanism is elaborated to deal with Cu. The increased expression of the mitochondrial ABC transporter Atm1 serves as a novel mechanism to cope with Cu stress by increasing the export of an Fe-S cluster precursor(s) so that essential cellular processes which depend on the activities of Fe-S proteins remain active during Cu stress. Indeed, while Atm1 depletion modestly reduced the virulence of the fungus in an intranasal model of cryptococcosis, activated macrophages were more efficient in containing the growth of cells with low levels of Atm1 than control cells. These results likely reflect the importance of Atm1, and of an arsenal of essential Fe-S proteins, for the fitness of the pathogen in an *in vivo* setting.

MATERIALS AND METHODS

Strains and media. *Cryptococcus neoformans* strains (see Table S1 in Text S1 in the supplemental material) were routinely grown at 30°C in synthetic complete (SC) medium (MP Biomedicals) containing either 2% glucose (SC or SC-gluc) or 2% galactose (SC-gal) or in yeast nitrogen base (YNB) medium containing either 2% glucose (YNB-gluc) or 2% galactose (YNB-gal), as indicated.

S. cerevisiae strains used in this study are listed in Table S1 in Text S1. Cells were cultivated in rich medium (YP) or SC supplemented with amino acids as required and 2% (wt/vol) glucose or galactose (65). Fe-depleted minimal medium was prepared using YNB without $FeCl_3$ (Formedium). Plasmids used in this study are listed in Table S2 in Text S1. Plasmid constructs were verified by DNA sequencing and/or functional complementation of a corresponding yeast mutant.

RNA isolation and qRT-PCR. *C. neoformans ATM1* expression was analyzed in wild-type and Δ*Cuf1* backgrounds as follows. Overnight cultures of *C. neoformans* in SC medium were inoculated into 5 ml fresh SC medium at an optical density at 600 nm (OD_{600}) of 0.3 and allowed to grow for 2 h at 30°C with shaking at 200 rpm. Cultures were then treated with either 1 mM Cu_2SO_4 or 1 mM BCS during 3 h. After the treatment, cells were pelleted and stored at −80°C prior to processing. For gene expression in Atm1-F and Gal7-Atm1-F strains, cells were back-diluted in either SC-gluc medium or SC-gal medium (as indicated) for three consecutive days. At day 3, cells were diluted (in each corresponding medium) to an OD_{600} of 0.3 and were allowed to grow for 2 h as described above. After the 2 h had elapsed, cells were either left untreated or treated with the indicated amounts of $CuSO_4$ for 3 h. Cells were then pelleted and stored at −80°C prior to processing. RNA was isolated from the stored pellets using a Qiagen RNeasy minikit, and DNase was treated with a Turbo DNA-free kit (Roche). Quantitative PCR (qPCR) was performed using specific primers for *ACT1*, *ATM1*, *CIG1*, *SIT1*, *MT1*, and *MT2* (primer sequences are described in Table S3 in Text S1) and iQ SYBR green Supermix (BioRad), and amplification and detection were performed using a CFX384 real-time system (BioRad), as previously described (66). Normalized expression levels were determined by calculating the threshold cycle ($\Delta\Delta C_T$) value for each gene in relation to *ACT1*.

Chromatin immunoprecipitation. Cells expressing Cuf1-FLAG were treated with 1 mM Cu or 1 mM BCS for 3 h. ChIP-PCR analysis was performed as described previously (9). Promoter sequences of *ATM1* and *TUB2* were analyzed by qPCR. The primers used are described in Table S3 in Text S1.

Protein extraction and Western blotting. For analyzing Atm1-FLAG expression, overnight SC cultures of *C. neoformans* were diluted to an OD_{600} of 0.3 in 5 ml of fresh SC media. Cells were grown for 2 h more and then treated with the indicated concentrations of Cu_2SO_4 for the indicated times. After each time point, 100% trichloroacetic acid (TCA) was added to the culture to reach a 10% concentration and cells were pelleted and collected with 20% TCA and stored at −20°C. To check the sugar-dependent expression of Atm1 and Leu1-HA expression after ZPT and/or Cu treatments in the Atm1-F and Gal7-Atm1-F strains, cells were back-diluted in either SC-gal or SC-gluc medium (as indicated) for three consecutive days (as indicated). At day 3, cells were diluted in 5 ml of fresh SC-gal or SC-gluc medium to an OD_{600} of 0.3. After 3 additional hours of growth, 100% TCA was added to reach a 10% final concentration and cells were collected and stored as described above. Stored pelleted cells were treated with 100 μl of 10% TCA, approximately 100 μl of glass beads was added, and the pellets were disrupted in a Mini-BeadBeater (BioSpec) using three sets of 1-min-ON and 1-min-OFF intervals. The whole-cell extract (without the beads) was transferred to a new tube, and the reaction mixture was centrifuged at maximum speed for 2 min in a microcentrifuge. The supernatant was discarded, and the cellular pellet was washed with 1 ml of ice-cold acetone. After 2 min of centrifugation, the acetone was eliminated and the pellet was dried and then resuspended in 80 μl of 100 mM Tris-HCl (pH 8.3)–1 mM EDTA–1% SDS. Samples were loaded in a gel and were analyzed with FLAG (monoclonal and horseradish peroxidase

[HRP] conjugated; Sigma-Aldrich), H3 (D1H2, polyclonal; Cell Signaling Technology, Inc.), HA (Y-11, polyclonal; Santa Cruz), Aco, or Cdc2 (monoclonal, anti-PSTAIR; Abcam, Inc.) antibodies.

Enzymatic activities. For measurement of enzymatic activities, cells were back-diluted in SC-gluc medium for three consecutive days. At day 3, cells were diluted to an OD_{600} of 0.3 in fresh SC-gluc media and were allowed to grow for 2 h. At that time point, cells were either left untreated or treated at the indicated concentrations of stressors for the indicated times, and the enzymatic activities were measured as previously described (67).

Microscopy. *C. neoformans* cells expressing or not expressing Atm1-mCherry from the *GAL7* promoter were back-diluted in SC-gal medium for three consecutive days. At day 3, cells were diluted to an OD_{600} of 0.3 in fresh SC-gal media and allowed to grow for 2 h. At that time point, cells were stained with Mitotracker green (Invitrogen) following the instructions of the manufacturer. Microscopy pictures were taken using a Zeiss 780 upright fixed-stage confocal microscope.

Growth curves. Quantitative growth analysis was performed to analyze the susceptibility of strains to stressors as follows. *C. neoformans* cultures were back-diluted during three consecutive days either in galactose (SC-gal or YNB-gal) or in glucose (SC-gluc or YNB-gluc) medium. At day 3, cells were diluted to an OD_{600} of 0.002, in fresh media, and were divided into aliquots and added to 96-well plates. Test compounds were added from fresh stock solutions of Cu_2SO_4 prepared in water and of 1-hydroxypyridine-2-thione zinc salt (zinc-pyrithione or ZPT) prepared in dimethyl sulfoxide (DMSO) (all products from Sigma-Aldrich), at the indicated concentrations. Plates were covered with a semipermeable membrane and incubated at 30°C with shaking at 900 rpm in a Finstruments shaker instrument. Growth graphs were generated by plotting the OD_{600} readings versus the compound concentrations at the 48-h time point.

Miscellaneous methods. The following published methods were used: manipulation of DNA and PCR (68); transformation of *S. cerevisiae* cells (69); determination of promoter strength using luciferase (67); and *in vivo* labeling of *C. neoformans* or *S. cerevisiae* cells with ^{55}FeCl (ICN) and measurement of ^{55}Fe incorporation into Fe-S proteins by immunoprecipitation and scintillation counting (67, 70). For *S. cerevisiae* Western blot analysis, antibodies were raised against recombinant purified proteins in rabbits. Antibodies against c-Myc or HA were obtained from Santa Cruz and protein A Sepharose from GE Healthcare.

Macrophage coculturing assay. The macrophage coculturing assay was performed as previously described (66). After 2 h of coinfection, nonphagocytosed *C. neoformans* cells were removed, and the remaining macrophages (containing or not containing *C. neoformans*) were washed 3 times with phosphate-buffered saline (PBS). Half of the coinfection cultures were plated for *C. neoformans* CFU at this point (the 2-h time point for calculating the phagocytosis index), and the other half were kept for an additional 24 h before plating for CFU (24-h time point for calculating the percentage of *C. neoformans* survival) was performed. *C. neoformans* cells for CFU were plated in SC-gal plates and incubated for up to 72 h at 30°C.

Mouse infection experiment. Female A/J mice (aged 4 to 6 weeks) were purchased from Jackson Laboratories. Mice were given a week to acclimate at the mouse facility. For the animal infection, the Atm1-F and the Gal7-Atm1-F strains were grown in SC-gluc medium for two consecutive days. At day 2, cells were washed with PBS three times and diluted to a cellular density of 4×10^6 cell/ml. Twenty-five microliters of this dilution was intranasally inoculated into mice that had previously been anesthetized in a manner consistent with IACUC standards. The mouse endpoint was considered a 15% reduction in weight.

Statistical analysis. In all figures, error bars represent statistical errors of the means (SEM) of results from a number of biological replicates (*n*), as indicated in the figure legends. The SEM was used because it provides a measurement of the accuracy of means of results of comparisons between different biological replicates. Before any statistical tests were conducted, data were log transformed for comparisons of proportions. The statistical tests chosen were paired *t* tests or analysis of variance (ANOVA) for repeated measures. The rationale for using paired and repeated-measures tests is that the experimental samples within a biological replicate are paired by experimental day. Data corresponding to results of statistical tests and the calculated *P* values are indicated in the figure legends. For those *P* values calculated with ANOVA which were significant, either the Bonferroni test or Fisher's least-significant-difference test was applied to find differences within the groups (multiple-comparison tests) and the data were labeled with asterisks corresponding to statistical significance as follows: ****, $P = <0.0001$; ***, $P = 0.0001$ to $P = <0.001$; **, $P = 0.001$ to $P = <0.01$; *, $P = 0.01$ to $P = <0.05$; ns (not significant), $P = >0.05$. Nonsignificant values are either not indicated or indicated for relevant experiments only.

SUPPLEMENTAL MATERIAL

Supplemental material for this article may be found at https://doi.org/10.1128/mBio.01742-17.

TEXT S1, PDF file, 0.3 MB.

FIG S1, TIF file, 0.3 MB.

FIG S2, TIF file, 0.1 MB.

FIG S3, TIF file, 0.1 MB.

FIG S4, TIF file, 0.1 MB.

FIG S5, TIF file, 0.1 MB.

FIG S6, TIF file, 0.1 MB.
FIG S7, TIF file, 0.2 MB.
FIG S8, TIF file, 0.02 MB.

ACKNOWLEDGMENTS

We thank Brandon L. Logeman and Aaron Smith for valuable comments on the manuscript. We thank Theodore Slotkin for valuable advice on statistical analysis of data.

This work was funded by a grant from the National Institutes of Health (R01GM041840) to D.J.T. and by generous financial support from Deutsche Forschungsgemeinschaft (Koselleck grant, LI 415/5, SFB 987) to R.L. The funders had no role in study design, data collection and interpretation of the results, or the decision to submit the work for publication.

REFERENCES

1. Alspaugh JA. 2015. Virulence mechanisms and Cryptococcus neoformans pathogenesis. Fungal Genet Biol 78:55–58. https://doi.org/10.1016/j.fgb.2014.09.004.
2. Heitman J, Kozel TR, Kwon-Chung KJ, Perfect JR, Casadevall A. 2011. Cryptococcus: from human pathogen to model yeast. American Society of Microbiology, Washington, DC. https://doi.org/10.1128/9781555816858.
3. Kronstad JW, Attarian R, Cadieux B, Choi J, D'Souza CA, Griffiths EJ, Geddes JM, Hu G, Jung WH, Kretschmer M, Saikia S, Wang J. 2011. Expanding fungal pathogenesis: Cryptococcus breaks out of the opportunistic box. Nat Rev Microbiol 9:193–203. https://doi.org/10.1038/nrmicro2522.
4. Park BJ, Wannemuehler KA, Marston BJ, Govender N, Pappas PG, Chiller TM. 2009. Estimation of the current global burden of cryptococcal meningitis among persons living with HIV/AIDS. AIDS 23:525–530. https://doi.org/10.1097/QAD.0b013e328322ffac.
5. Chang YC, Kwon-Chung KJ. 1994. Complementation of a capsule-deficient mutation of Cryptococcus neoformans restores its virulence. Mol Cell Biol 14:4912–4919. https://doi.org/10.1128/MCB.14.7.4912.
6. Cox GM, Mukherjee J, Cole GT, Casadevall A, Perfect JR. 2000. Urease as a virulence factor in experimental cryptococcosis. Infect Immun 68:443–448. https://doi.org/10.1128/IAI.68.2.443-448.2000.
7. Kronstad J, Saikia S, Nielson ED, Kretschmer M, Jung W, Hu G, Geddes JM, Griffiths EJ, Choi J, Cadieux B, Caza M, Attarian R. 2012. Adaptation of Cryptococcus neoformans to mammalian hosts: integrated regulation of metabolism and virulence. Eukaryot Cell 11:109–118. https://doi.org/10.1128/EC.05273-11.
8. Salas SD, Bennett JE, Kwon-Chung KJ, Perfect JR, Williamson PR. 1996. Effect of the laccase gene CNLAC1, on virulence of Cryptococcus neoformans. J Exp Med 184:377–386. https://doi.org/10.1084/jem.184.2.377.
9. Ding C, Festa RA, Chen YL, Espart A, Palacios Ò, Espín J, Capdevila M, Atrian S, Heitman J, Thiele DJ. 2013. Cryptococcus neoformans copper detoxification machinery is critical for fungal virulence. Cell Host Microbe 13:265–276. https://doi.org/10.1016/j.chom.2013.02.002.
10. Sun TS, Ju X, Gao HL, Wang T, Thiele DJ, Li JY, Wang ZY, Ding C. 2014. Reciprocal functions of Cryptococcus neoformans copper homeostasis machinery during pulmonary infection and meningoencephalitis. Nat Commun 5:5550. https://doi.org/10.1038/ncomms6550.
11. García-Santamarina S, Thiele DJ. 2015. Copper at the fungal pathogen-host axis. J Biol Chem 290:18945–18953. https://doi.org/10.1074/jbc.R115.649129.
12. Cox GM, Harrison TS, McDade HC, Taborda CP, Heinrich G, Casadevall A, Perfect JR. 2003. Superoxide dismutase influences the virulence of Cryptococcus neoformans by affecting growth within macrophages. Infect Immun 71:173–180. https://doi.org/10.1128/IAI.71.1.173-180.2003.
13. Dickinson EK, Adams DL, Schon EA, Glerum DM. 2000. A human SCO_2 mutation helps define the role of Sco1p in the cytochrome oxidase assembly pathway. J Biol Chem 275:26780–26785. https://doi.org/10.1074/jbc.M004032200.
14. Jung WH, Sham A, Lian T, Singh A, Kosman DJ, Kronstad JW. 2008. Iron source preference and regulation of iron uptake in Cryptococcus neoformans. PLoS Pathog 4:e45. https://doi.org/10.1371/journal.ppat.0040045.
15. Walton FJ, Idnurm A, Heitman J. 2005. Novel gene functions required for melanization of the human pathogen Cryptococcus neoformans. Mol Microbiol 57:1381–1396. https://doi.org/10.1111/j.1365-2958.2005.04779.x.
16. Williamson PR. 1994. Biochemical and molecular characterization of the diphenol oxidase of Cryptococcus neoformans: identification as a laccase. J Bacteriol 176:656–664. https://doi.org/10.1128/jb.176.3.656-664.1994.
17. Ding C, Yin J, Tovar EM, Fitzpatrick DA, Higgins DG, Thiele DJ. 2011. The copper regulon of the human fungal pathogen Cryptococcus neoformans H99. Mol Microbiol 81:1560–1576. https://doi.org/10.1111/j.1365-2958.2011.07794.x.
18. Waterman SR, Hacham M, Hu G, Zhu X, Park YD, Shin S, Panepinto J, Valyi-Nagy T, Beam C, Husain S, Singh N, Williamson PR. 2007. Role of a CUF1/CTR4 copper regulatory axis in the virulence of Cryptococcus neoformans. J Clin Invest 117:794–802. https://doi.org/10.1172/JCI30006.
19. Wagner D, Maser J, Lai B, Cai Z, Barry CE III, Höner Zu Bentrup K, Russell DG, Bermudez LE. 2005. Elemental analysis of Mycobacterium avium-, Mycobacterium tuberculosis-, and Mycobacterium smegmatis-containing phagosomes indicates pathogen-induced microenvironments within the host cell's endosomal system. J Immunol 174:1491–1500. https://doi.org/10.4049/jimmunol.174.3.1491.
20. White C, Lee J, Kambe T, Fritsche K, Petris MJ. 2009. A role for the ATP7A copper-transporting ATPase in macrophage bactericidal activity. J Biol Chem 284:33949–33956. https://doi.org/10.1074/jbc.M109.070201.
21. Achard ME, Tree JJ, Holden JA, Simpfendorfer KR, Wijburg OL, Strugnell RA, Schembri MA, Sweet MJ, Jennings MP, McEwan AG. 2010. The multi-copper-ion oxidase CueO of Salmonella enterica serovar Typhimurium is required for systemic virulence. Infect Immun 78:2312–2319. https://doi.org/10.1128/IAI.01208-09.
22. Wiemann P, Perevitsky A, Lim FY, Shadkchan Y, Knox BP, Landero Figueora JA, Choera T, Niu M, Steinberger AJ, Wüthrich M, Idol RA, Klein BS, Dinauer MC, Huttenlocher A, Osherov N, Keller NP. 2017. Aspergillus fumigatus copper export machinery and reactive oxygen intermediate defense counter host copper-mediated oxidative antimicrobial offense. Cell Rep 19:1008–1021. https://doi.org/10.1016/j.celrep.2017.04.019.
23. Wolschendorf F, Ackart D, Shrestha TB, Hascall-Dove L, Nolan S, Lamichhane G, Wang Y, Bossmann SH, Basaraba RJ, Niederweis M. 2011. Copper resistance is essential for virulence of Mycobacterium tuberculosis. Proc Natl Acad Sci U S A 108:1621–1626. https://doi.org/10.1073/pnas.1009261108.
24. Macomber L, Imlay JA. 2009. The iron-sulfur clusters of dehydratases are primary intracellular targets of copper toxicity. Proc Natl Acad Sci U S A 106:8344–8349. https://doi.org/10.1073/pnas.0812808106.
25. Macomber L, Rensing C, Imlay JA. 2007. Intracellular copper does not catalyze the formation of oxidative DNA damage in Escherichia coli. J Bacteriol 189:1616–1626. https://doi.org/10.1128/JB.01357-06.
26. Tan G, Cheng Z, Pang Y, Landry AP, Li J, Lu J, Ding H. 2014. Copper binding in IscA inhibits iron-sulphur cluster assembly in Escherichia coli. Mol Microbiol 93:629–644. https://doi.org/10.1111/mmi.12676.
27. Chillappagari S, Seubert A, Trip H, Kuipers OP, Marahiel MA, Miethke M. 2010. Copper stress affects iron homeostasis by destabilizing iron-sulfur cluster formation in Bacillus subtilis. J Bacteriol 192:2512–2524. https://doi.org/10.1128/JB.00058-10.
28. Brancaccio D, Gallo A, Piccioli M, Novellino E, Ciofi-Baffoni S, Banci L.

2017. [4Fe-4S] cluster assembly in mitochondria and its impairment by copper. J Am Chem Soc 139:719–730. https://doi.org/10.1021/jacs.6b09567.
29. Kispal G, Csere P, Guiard B, Lill R. 1997. The ABC transporter Atm1p is required for mitochondrial iron homeostasis. FEBS Lett 418:346–350. https://doi.org/10.1016/S0014-5793(97)01414-2.
30. Kispal G, Csere P, Prohl C, Lill R. 1999. The mitochondrial proteins Atm1p and Nfs1p are essential for biogenesis of cytosolic Fe/S proteins. EMBO J 18:3981–3989. https://doi.org/10.1093/emboj/18.14.3981.
31. Srinivasan V, Pierik AJ, Lill R. 2014. Crystal structures of nucleotide-free and glutathione-bound mitochondrial ABC transporter Atm1. Science 343:1137–1140. https://doi.org/10.1126/science.1246729.
32. Lill R, Srinivasan V, Mühlenhoff U. 2014. The role of mitochondria in cytosolic-nuclear iron–sulfur protein biogenesis and in cellular iron regulation. Curr Opin Microbiol 22:111–119. https://doi.org/10.1016/j.mib.2014.09.015.
33. Lill R, Kispal G. 2001. Mitochondrial ABC transporters. Res Microbiol 152:331–340. https://doi.org/10.1016/S0923-2508(01)01204-9.
34. Hausmann A, Samans B, Lill R, Mühlenhoff U. 2008. Cellular and mitochondrial remodeling upon defects in iron-sulfur protein biogenesis. J Biol Chem 283:8318–8330. https://doi.org/10.1074/jbc.M705570200.
35. Lill R, Dutkiewicz R, Freibert SA, Heidenreich T, Mascarenhas J, Netz DJ, Paul VD, Pierik AJ, Richter N, Stümpfig M, Srinivasan V, Stehling O, Mühlenhoff U. 2015. The role of mitochondria and the CIA machinery in the maturation of cytosolic and nuclear iron-sulfur proteins. Eur J Cell Biol 94:280–291. https://doi.org/10.1016/j.ejcb.2015.05.002.
36. Mühlenhoff U, Hoffmann B, Richter N, Rietzschel N, Spantgar F, Stehling O, Uzarska MA, Lill R. 2015. Compartmentalization of iron between mitochondria and the cytosol and its regulation. Eur J Cell Biol 94:292–308. https://doi.org/10.1016/j.ejcb.2015.05.003.
37. Jung WH, Sham A, White R, Kronstad JW. 2006. Iron regulation of the major virulence factors in the AIDS-associated pathogen Cryptococcus neoformans. PLoS Biol 4:e410. https://doi.org/10.1371/journal.pbio.0040410.
38. Leighton J, Schatz G. 1995. An ABC transporter in the mitochondrial inner membrane is required for normal growth of yeast. EMBO J 14:188–195.
39. Chloupková M, LeBard LS, Koeller DM. 2003. MDL1 is a high copy suppressor of ATM1: evidence for a role in resistance to oxidative stress. J Mol Biol 331:155–165. https://doi.org/10.1016/S0022-2836(03)00666-1.
40. Cerda BA, Wesdemiotis C. 1995. The relative copper(I) ion affinities of amino acids in the gas phase. J Am Chem Soc 117:9734–9739. https://doi.org/10.1021/ja00143a017.
41. Gruer MJ, Artymiuk PJ, Guest JR. 1997. The aconitase family: three structural variations on a common theme. Trends Biochem Sci 22:3–6. https://doi.org/10.1016/S0968-0004(96)10069-4.
42. Karcher A, Schele A, Hopfner KP. 2008. X-ray structure of the complete ABC enzyme ABCE1 from Pyrococcus abyssi. J Biol Chem 283:7962–7971. https://doi.org/10.1074/jbc.M707347200.
43. Stehling O, Wilbrecht C, Lill R. 2014. Mitochondrial iron-sulfur protein biogenesis and human disease. Biochimie 100:61–77. https://doi.org/10.1016/j.biochi.2014.01.010.
44. Lloyd SJ, Lauble H, Prasad GS, Stout CD. 1999. The mechanism of aconitase: 1.8 A resolution crystal structure of the S642a:citrate complex. Protein Sci 8:2655–2662. https://doi.org/10.1110/ps.8.12.2655.
45. Chaikuad A, Johansson C, Krojer T, Yue WW, Phillips C, Bray JE, Pike ACW, Muniz JRC, Vollmar M, Weigelt J, Arrowsmith CH, Edwards AM, Bountra C, Kavanagh K, Oppermann U; Structural Genomics Consortium (SGC). 2010. Crystal structure of human ferredoxin-1 (FDX1) in complex with iron-sulfur cluster. https://doi.org/10.2210/pdb3p1m/pdb.
46. Vallières C, Holland SL, Avery SV. 31 August 2017. Mitochondrial ferredoxin determines vulnerability of cells to copper excess. Cell Chem Biol https://doi.org/10.1016/j.chembiol.2017.08.005.
47. Mühlenhoff U, Gerber J, Richhardt N, Lill R. 2003. Components involved in assembly and dislocation of iron-sulfur clusters on the scaffold protein Isu1p. EMBO J 22:4815–4825. https://doi.org/10.1093/emboj/cdg446.
48. Netz DJ, Mascarenhas J, Stehling O, Pierik AJ, Lill R. 2014. Maturation of cytosolic and nuclear iron-sulfur proteins. Trends Cell Biol 24:303–312. https://doi.org/10.1016/j.tcb.2013.11.005.
49. Netz DJ, Genau HM, Weiler BD, Bill E, Pierik AJ, Lill R. 2016. The conserved protein Dre2 uses essential [2Fe-2S] and [4Fe-4S] clusters for its function in cytosolic iron-sulfur protein assembly. Biochem J 473:2073–2085. https://doi.org/10.1042/BCJ20160416.
50. Netz DJ, Pierik AJ, Stümpfig M, Bill E, Sharma AK, Pallesen LJ, Walden WE, Lill R. 2012. A bridging [4Fe-4S] cluster and nucleotide binding are essential for function of the Cfd1-Nbp35 complex as a scaffold in iron-sulfur protein maturation. J Biol Chem 287:12365–12378. https://doi.org/10.1074/jbc.M111.328914.
51. Urzica E, Pierik AJ, Mühlenhoff U, Lill R. 2009. Crucial role of conserved cysteine residues in the assembly of two iron-sulfur clusters on the CIA protein Nar1. Biochemistry 48:4946–4958. https://doi.org/10.1021/bi900312x.
52. Mühlenhoff U, Molik S, Godoy JR, Uzarska MA, Richter N, Seubert A, Zhang Y, Stubbe J, Pierrel F, Herrero E, Lillig CH, Lill R. 2010. Cytosolic monothiol glutaredoxins function in intracellular iron sensing and trafficking via their bound iron-sulfur cluster. Cell Metab 12:373–385. https://doi.org/10.1016/j.cmet.2010.08.001.
53. Iwema T, Picciocchi A, Traore DA, Ferrer JL, Chauvat F, Jacquamet L. 2009. Structural basis for delivery of the intact [Fe2S2] cluster by monothiol glutaredoxin. Biochemistry 48:6041–6043. https://doi.org/10.1021/bi900440m.
54. Poor CB, Wegner SV, Li H, Dlouhy AC, Schuermann JP, Sanishvili R, Hinshaw JR, Riggs-Gelasco PJ, Outten CE, He C. 2014. Molecular mechanism and structure of the Saccharomyces cerevisiae iron regulator Aft2. Proc Natl Acad Sci U S A 111:4043–4048. https://doi.org/10.1073/pnas.1318869111.
55. Rutherford JC, Ojeda L, Balk J, Mühlenhoff U, Lill R, Winge DR. 2005. Activation of the iron regulon by the yeast Aft1/Aft2 transcription factors depends on mitochondrial but not cytosolic iron-sulfur protein biogenesis. J Biol Chem 280:10135–10140. https://doi.org/10.1074/jbc.M413731200.
56. Andrew AJ, Song JY, Schilke B, Craig EA. 2008. Posttranslational regulation of the scaffold for Fe-S cluster biogenesis, Isu. Mol Biol Cell 19:5259–5266. https://doi.org/10.1091/mbc.E08-06-0622.
57. Ciesielski SJ, Schilke B, Marszalek J, Craig EA. 2016. Protection of scaffold protein Isu from degradation by the Lon protease Pim1 as a component of Fe-S cluster biogenesis regulation. Mol Biol Cell 27:1060–1068. https://doi.org/10.1091/mbc.E15-12-0815.
58. Li H, Stümpfig M, Zhang C, An X, Stubbe J, Lill R, Huang M. 2017. The diferric-tyrosyl radical cluster of ribonucleotide reductase and cytosolic iron-sulfur clusters have distinct and similar biogenesis requirements. J Biol Chem 292:11445–11451. https://doi.org/10.1074/jbc.M117.786178.
59. Reeder NL, Kaplan J, Xu J, Youngquist RS, Wallace J, Hu P, Juhlin KD, Schwartz JR, Grant RA, Fieno A, Nemeth S, Reichling T, Tiesman JP, Mills T, Steinke M, Wang SL, Saunders CW. 2011. Zinc pyrithione inhibits yeast growth through copper influx and inactivation of iron-sulfur proteins. Antimicrob Agents Chemother 55:5753–5760. https://doi.org/10.1128/AAC.00724-11.
60. Reeder NL, Xu J, Youngquist RS, Schwartz JR, Rust RC, Saunders CW. 2011. The antifungal mechanism of action of zinc pyrithione. Br J Dermatol 165(Suppl 2):9–12. https://doi.org/10.1111/j.1365-2133.2011.10571.x.
61. Lill R, Hoffmann B, Molik S, Pierik AJ, Rietzschel N, Stehling O, Uzarska MA, Webert H, Wilbrecht C, Mühlenhoff U. 2012. The role of mitochondria in cellular iron-sulfur protein biogenesis and iron metabolism. Biochim Biophys Acta 1823:1491–1508. https://doi.org/10.1016/j.bbamcr.2012.05.009.
62. Alhebshi A, Sideri TC, Holland SL, Avery SV. 2012. The essential iron-sulfur protein Rli1 is an important target accounting for inhibition of cell growth by reactive oxygen species. Mol Biol Cell 23:3582–3590. https://doi.org/10.1091/mbc.E12-05-0413.
63. Paul VD, Mühlenhoff U, Stümpfig M, Seebacher J, Kugler KG, Renicke C, Taxis C, Gavin AC, Pierik AJ, Lill R. 2015. The deca-GX3 proteins Yae1-Lto1 function as adaptors recruiting the ABC protein Rli1 for iron-sulfur cluster insertion. Elife 4:e08231. https://doi.org/10.7554/eLife.08231.
64. Palacios Ò, Espart A, Espín J, Ding C, Thiele DJ, Atrian S, Capdevila M. 2014. Full characterization of the Cu-, Zn-, and Cd-binding properties of CnMT1 and CnMT2, two metallothioneins of the pathogenic fungus Cryptococcus neoformans acting as virulence factors. Metallomics 6:279–291. https://doi.org/10.1039/c3mt00266g.
65. Sherman F. 2002. Getting started with yeast. Methods Enzymol 350:3–41. https://doi.org/10.1016/S0076-6879(02)50954-X.
66. Festa RA, Helsel ME, Franz KJ, Thiele DJ. 2014. Exploiting innate immune cell activation of a copper-dependent antimicrobial agent during infection. Chem Biol 21:977–987. https://doi.org/10.1016/j.chembiol.2014.06.009.

67. Molik S, Lill R, Mühlenhoff U. 2007. Methods for studying iron metabolism in yeast mitochondria. Methods Cell Biol 80:261–280. https://doi.org/10.1016/S0091-679X(06)80013-0.
68. Sambrook J, Russell DW. 2001. Molecular cloning: a laboratory manual, 3rd ed. Cold Spring Harbor Press, Cold Spring Harbor, NY.
69. Gietz RD, Woods RA. 2002. Transformation of yeast by lithium acetate/single-stranded carrier DNA/polyethylene glycol method. Methods Enzymol 350:87–96. https://doi.org/10.1016/S0076-6879(02)50957-5.
70. Pierik AJ, Netz DJA, Lill R. 2009. Analysis of iron-sulfur protein maturation in eukaryotes. Nat Protoc 4:753–766. https://doi.org/10.1038/nprot.2009.39.